A novel method for detecting sit-to-stand intent using mechanical toe stimulus with foot reaction forces

Jian Zheng[1], Ming Jiang[1] , Qizhi Meng[1], Yusuke Sugahara[1], Marco Ceccarelli[2,3] and Yukio Takeda[1]

[1]Department of Mechanical Engineering, Institute of Science Tokyo, Tokyo, Japan
[2]IRFI, School of Engineering, Institute of Science Tokyo, Tokyo, Japan
[3]Department of Industrial Engineering, University of Rome Tor Vergata, Roma, Italy
Corresponding author: Ming Jiang; Email: jiang.m.889e@m.isct.ac.jp

Abstract

Sit-to-stand (STS) motion is an essential daily activity. However, this motion becomes increasingly difficult for older adults as their muscle strength declines with age. To assist individuals in standing up while maximizing their muscle strength based on the assist-as-needed (AAN) strategy, assistive devices must detect early STS intent, specifically before the buttocks leave the chair, to ensure timely assistance. This study proposes a novel method for detecting STS intent by applying external mechanical stimuli to the toes and analyzing the resulting changes in heel and toe-reaction forces. Moreover, a structured detection framework was developed by utilizing predefined thresholds for the change rate and magnitude of the heel and toe-reaction forces to detect STS intent. Offline tests for threshold setting of STS-intent detection were established in the offline tests: change rate and magnitude of the reaction forces on the heel and toes. The thresholds for each criterion were determined using the Pareto optimization method. Using the determined thresholds, these criteria were then applied in online tests to evaluate the performance of the proposed intent detection method. The results demonstrated that mechanical stimuli improved the performance of STS-intent detection, providing accurate and stable detection. This method can be applied to STS-assistive devices to effectively implement AAN functionality for standing assistance.

1. Introduction

Sit-to-stand (STS) is a fundamental activity that is frequently performed in daily life. This motion is an important step before engaging in other activities, such as transitioning from sitting to walking, using the toilet, and going outdoors, which significantly impacts quality of life (QoL). However, in an aging society, a growing number of elderly adults with muscle weakness experiences difficulties in standing [1]. The lower extremity strength of older adults is approximately 50% of that of younger adults [2]. Therefore, caregivers must assist elderly adults with their daily activities. However, relying solely on human assistance burdens caregivers with physical and emotional stress. Moreover, the lack of workforce, risk of workplace injuries, and increasing demand for elderly care further highlight the limitations of caregiving methods that rely on human assistance. To address these problems and improve the QoL of older adults, the utilization of assistive robots for standing assistance has been increasingly explored as a promising solution [3–5]. However, excessive assistance may reduce the user's engagement in STS motion, potentially leading to muscle disuse and decreased physical function. To address this drawback, some studies [6–8] have proposed an assist-as-needed (AAN) approach. This approach aims to assist users in standing while encouraging them to use their strength as much as possible, thereby promoting muscle activation. During the STS procedure, when users attempt to stand with

their strengths, it is necessary to provide timely assistance if they cannot stand independently. Without timely assistance, users may struggle to complete their motions or even risk falling. Approximately, 30% of community-dwelling individuals aged $\geq$ 65 years experience at least one fall annually, with this proportion increasing to 50% by the age of 80 [9]. Therefore, accurately detecting STS intention at an early phase of motion, specifically before the buttocks leave the chair, is crucial for ensuring timely assistance, reducing the risk of falls, and encouraging users to effectively engage their strength during STS motion.

Various assistive devices have been developed to assist with STS motion. For example, Shepherd et al. developed a knee exoskeleton to assist stroke patients with STS motion [10]. Jeong et al. developed a four-bar linkage mechanism for a chair system to assist with STS motion [11]. These studies provided full assistance to the STS motion without considering the user's physical condition [12]. In addition, several STS-assistive devices feature AAN functionality, which prevents over-reliance and further weakening of muscle strength. For example, in ref. [6], Wang et al. proposed a method for adjusting the assistance force provided by an STS-assist robot through parameter tuning, allowing it to better meet the needs of different older adults. Similarly, in ref. [7], Chugo et al. proposed an STS-assist walker robot for patients with care levels 1 or 2 under Japan's long-term care insurance system [13]. This robot enables patients to perform voluntary movements within a safe range, using only their muscle strength. Furthermore, in ref. [8], Naghavi et al. introduced an AAN control strategy for a hip exoskeleton that adjusted assistance based on a novel strength index. This strategy further improves patient engagement by minimizing unnecessary robotic interventions.

Although previous AAN-based approaches primarily focused on providing adaptive assistance tailored to user needs, the ability of these systems to accurately detect STS intent early in motion has not been addressed yet. In particular, it is necessary to provide timely and safe assistance before the buttocks leave the chair to encourage more active user participation. Common approaches for detecting STS intent involve measuring the angle of forward trunk inclination (AFI) and lower-limb electromyography (EMG) signals. In ref. [14], Li et al. combined AFI and EMG data from the quadriceps and established specific thresholds to detect STS intent. Their system achieved false acceptance and false rejection rates of less than 5%. When their system detected that an elderly individual in need of care was attempting to stand, it triggered an alarm to notify the caregivers, helping to prevent falls. Similarly, in ref. [15], Inoue et al. developed a system to predict STS speed by analyzing AFI and EMG data to provide timely support. In ref. [16], Hiyama et al. utilized EMG data from lower-limb muscle activation sequences to detect STS intent, predicting the user's intent approximately 130.4 ms before the buttocks left the chair. They successfully integrated this intention-detection method into a chair-type assistive system to support STS movements and reduce muscle effort. In [17], Yuan et al. developed an STS-intent detection method using EMG signals and employed a Kalman Filter to reduce the response time to 20 ms. This enables assistive robots to respond quickly and accurately to user movements, thereby improving the overall system performance.

Although the combination of AFI and EMG data has demonstrated impressive accuracy and fast response times for detecting STS intent, several practical challenges persist in daily applications. One concern is the inconsistency of the EMG signals, which can fluctuate based on the user's physical condition. Factors such as muscle fatigue and sweat interference can hinder reliable data collection and analysis [18]. EMG sensors, which are typically attached directly to the user's skin, can be inconvenient and intrusive in daily activities, such as changing clothes or showering, and may also place a physical burden on the user owing to prolonged wear. In addition to EMG-based approaches, pressure sensor-based methods have been investigated for STS detection. For example, in ref. [19, 20] Arcelus et al. utilized bed pressure sensors to measure STS timing and symmetry and detect anomalies such as bouncing. These methods face challenges, such as delayed detection and false alarms, which limit their practical application. Therefore, this study aimed to develop a method that can accurately and rapidly detect STS intent without burdening users and is simple to operate.

2. STS-intent detection using mechanical stimulus

Detecting STS intentions can be challenging, particularly when users are seated. Previous studies have utilized human–machine interactions to detect STS intent. In ref. [21], Cao et al. developed an STS rehabilitation robot that employs a double-rope system to assist users. The robot utilized the tensile forces of the ropes to detect the STS intent, where a decrease in tensile force indicated the user's intent to stand up, and an increase suggested the intent to sit down. In ref. [22], Tsusaka et al. improved assistive device technology by integrating the interaction forces between the user and robot, reflecting the dynamic adjustments observed between physiotherapists and patients. Their development focused on a feedback mechanism in robotic systems that adaptively adjusted the support based on the user's real-time forces, enhancing the smoothness and effectiveness of STS movements. Therefore, utilizing the interaction forces between humans and machines to detect the user intent has significant potential in assistive robotics. However, most current studies rely on a passive approach, in which robots infer their intent by observing changes in user movements. While this is effective, it may lack active engagement and may not provide the precision required for seamless human–robot interactions.

To address these potential limitations, we propose a novel approach in which robots actively apply a mechanical stimulus to the user and analyze the resulting changes in the reaction forces to detect STS intent. This method aims to enhance the interactivity of human–robot systems and may help users prepare psychologically for robotic assistance. We hypothesize that users' response behaviors to the applied stimulus will effectively reflect their intent, thereby enabling more accurate and stable intent detection. The concept of using physical stimuli to analyze user responses has been explored in previous studies. For example, in ref. [23], Bell and Asada developed a system to estimate the mental state of users by assessing whether they agreed to and accepted a robotic aid for safe and effective STS assistance. Their approach involved applying a light physical push to the user's back to prompt forward bending and analyzing their physical responses, such as shoulder movement direction and speed, to detect their willingness to cooperate with the robotic system.

In the context of the STS motion, determining the appropriate timing and method for applying a stimulus and interpreting the user's response as an indicator of intent are important factors to consider. STS motion can be divided into four phases [24], as shown in Figure 1. During the initial momentum transfer phase, as shown in Figure 1(b), the forward inclination of the trunk decreases the AFI and increases the ground reaction force (F_{feet}). These characteristic changes suggest that they can be used as indicators of STS intent.

To explore effective detection methods, the forward-direction force applied to the user's trunk during the seating phase (Figure 1(a)) can be considered a mechanical stimulus. For example, as hypothesized in this study, if a user responds to a stimulus with a forward movement, it may indicate an intention to stand, as shown in Figure 2. Conversely, if the user resists or does not respond to an applied stimulus, this may suggest that they have no intention of standing. However, this approach can be reconsidered because of several limitations. First, the forward inclination of the trunk is not limited to standing up; it frequently occurs in other everyday situations, such as reaching for objects or picking items up from the ground. A high frequency of forward inclinations can reduce the success rate of STS-intent detection. Second, mounting the mechanism on the trunk is challenging. Most importantly, if the user has no intention of standing, applying this mechanical stimulus can lead to loss of balance.

Alternatively, a mechanical stimulus applied to the toes can serve as a cue for detecting STS intent. Compared with situations without the intent to stand, F_{feet} increases significantly during STS motion, making it feasible to detect STS intent through changes in this reaction force. To validate this approach, as shown in Figure 1(b), the heel reaction force (F_{heel}) and toe-reaction force (F_{toe}) were used to represent F_{feet}. As shown in Figure 3, we hypothesize the following mechanism for detecting STS intent. When the toe-lifting stimulus pushes the toes upward – opposite to the direction of rising – a participant who intends to stand will exert a compensatory force to counter this stimulus, resulting in a marked increase in both F_{heel} and F_{toe}. Two factors are expected to contribute to the increase in F_{toe}: (1) passive viscoelastic responses of the ankle and foot structures, and (2) actively applied downward force associated
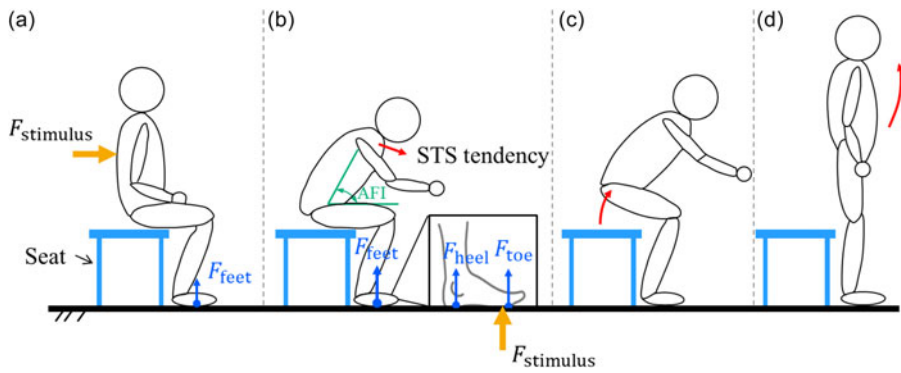
Figure 1. *Typical four phases of STS motion: (a) Seating phase, (b) Momentum transfer phase, (c) Extension phase, and (d) Stabilization phase.*
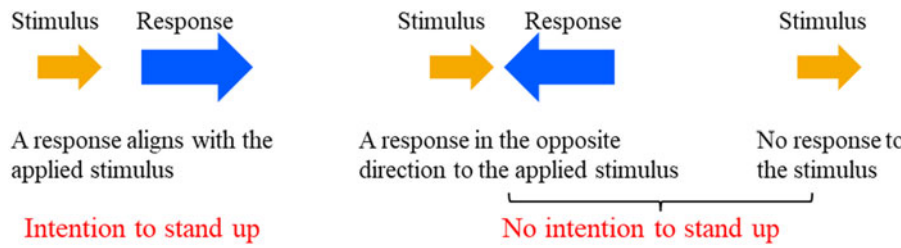

Figure 2. *Schematic of the two STS-intent states based on responses to a mechanical stimulus applied to the back. (The yellow arrow indicates the direction and magnitude of the mechanical stimulus, whereas the blue arrow represents the direction and magnitude of the user's response).*
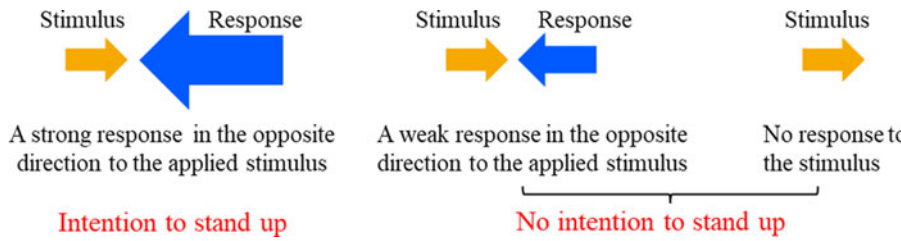

Figure 3. *Schematic of the two STS-intent states based on responses to a mechanical stimulus applied to the toes. (The yellow arrow indicates the direction and magnitude of the mechanical stimulus, and the blue arrow represents the direction and magnitude of the user's response to the stimulus).*

with preparation for the STS motion. Collectively, these passive and active components are expected to generate a larger increase in F_{toe} than either component would alone, making the force change a reliable indicator of STS intent. Accordingly, STS intent can be detected by setting predefined thresholds for F_{heel} and F_{toe}. Specifically, if the measured values exceed these thresholds, STS intent is identified; otherwise, it is concluded that there is no intention to stand. This method was selected in this study because of its several advantages. First, foot movements occur far less frequently than forward trunk inclinations in daily life. Second, the changes in the ground reaction force during STS motion were more pronounced. In addition, placing the stimulus device under the foot rather than attaching it to the body imposes a relatively small burden on users.

Based on the above hypothesis, we propose a method for detecting STS intent that utilizes an external stimulus to the user's toes when an STS motion is anticipated by analyzing the resulting reaction forces.

In our preliminary studies, we demonstrated that the magnitudes of AFI and F_{heel} could be used as trigger conditions for applying an external mechanical stimulus to improve the detection rate. By manually setting thresholds, the STS intent was successfully detected before the buttocks left the chair, while effectively distinguishing other interfering motions [25]. Further analysis revealed that AFI had a minimal impact on the detection algorithm. Therefore, further investigations were conducted on the feasibility of detecting STS intent using only the ground reaction force to improve usability. These experiments also employed manually set thresholds and successfully detected STS intent [26]. The Pareto optimization method was employed to enhance its practicality, enabling the automatic setting of thresholds when detecting STS intent, and its reliability was confirmed [27]. Expanding on this groundwork, this study conducted comprehensive experiments involving five subjects to systematically compare the detection performance under conditions with and without external mechanical stimuli. Using thresholds determined via the Pareto optimization method, this study evaluated the impact of the proposed method on detection accuracy, stability, and the trade-off between early detection and robustness.

3. Experimental setup and STS-intent detection methods

3.1. Experimental setup designed to investigate the effect of mechanical stimulus on detecting STS intent

The experimental setup used to investigate the effect of mechanical stimuli on the detection of STS intent is shown in Figure 4(a). The main components of the system include a seat equipped with a load cell (CZL601AC, YOLO LOADCELL), which was used to detect the instant at which the buttocks left the seat (indicated by the descent of the measured value at zero). A specially designed toe pedal was positioned under the user's foot to provide a mechanical stimulus to the toes. The detailed design is shown in Figure 4(b). The pedal was driven by a DC motor (540K75, TAMIYA Co., Ltd.), and two force sensors (USL08-H6-2KN, Tec Gihan Co., Ltd.) were installed in the heel and toe areas to continuously measure the applied forces. The positions of the two force sensors were determined based on the average foot length of individuals in Japan [28]. The subjects could adjust their foot position relative to their foot length such that only the heel and toe regions contacted the sensors, whereas the arch did not touch the sensors. This configuration enables accurate measurement of the ground reaction forces from a single foot. The motor operation and data-acquisition processes were controlled using an Arduino controller (Mega 2560) with a sampling time of 10 ms.

3.2. Detection strategies and experimental design

This study hypothesizes that the ground reaction force changes more rapidly and has a higher value when the subject intends to stand than when they do not. To detect STS intent, optimal thresholds were established to delineate the boundary between intending and not intending to stand. In the first step, offline tests were conducted to gather data and determine the optimal threshold for the correct detection of STS intent. In the second step, the determined thresholds were applied to online tests to evaluate detection performance. To simulate real-life scenarios, a normal STS motion (standing up) was performed to represent cases with STS intent, whereas two interfering motions were performed to represent cases without STS intent, as shown in Figure 5.

Without a stimulus, the ground reaction forces were measured without pedal rotation, as shown in Figure 6(a). In contrast, for the stimulus proposed in this study, when F_{heel} increases, indicating a potential intention to stand, a mechanical stimulus is applied to the toes of the user, as shown in Figure 6(b). This study conducted a comparative experiment to assess the performance of STS-intent detection with and without-stimulus conditions. The results were analyzed to evaluate the effects of the application of mechanical stimuli.

The process for providing the stimulus is illustrated in the flowchart shown in Figure 7. It commences with the system measuring the F_{heel}, F_{toe}, and the motor angle (θ_{motor}). When the subject was seated,
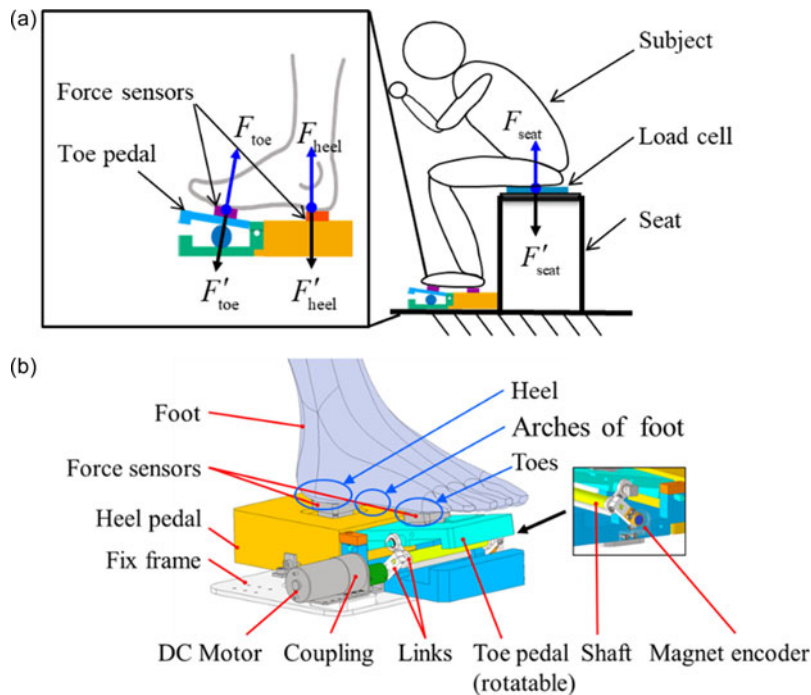
Figure 4. *Experimental setup to investigate the effect of mechanical stimulus on detecting STS intent: (a) Schematic of the experimental setup for detecting STS intent. (b) Mechanical design for applying mechanical stimulus to the toes of a single foot. F_{heel}: Heel reaction force applied to the heel. F'_{heel}: F_{heel}'s counterforce applied to the heel pedal. F_{toe}: Toe reaction force applied to the toes. F'_{toe}: F_{toe}'s counterforce applied to the toe pedal. F_{seat}: Seat reaction force to the participant. F'_{seat}: F_{seat}'s counterforce applied to the seat surface.*
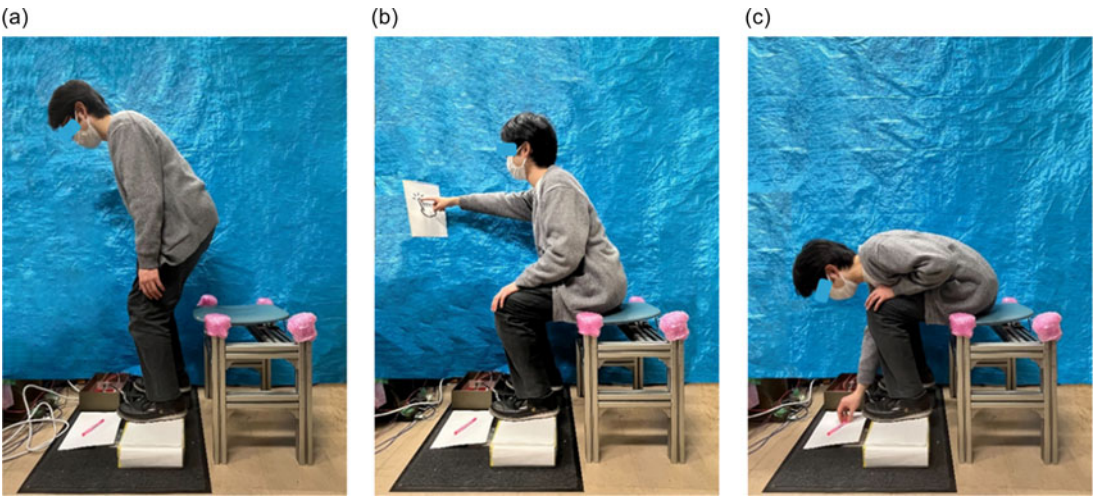

Figure 5. *Demonstration of normal STS motion and two types of interfering motions performed in the experiment: (a) normal STS motion, (b) grabbing items in front, and (c) picking up an item from the ground.*
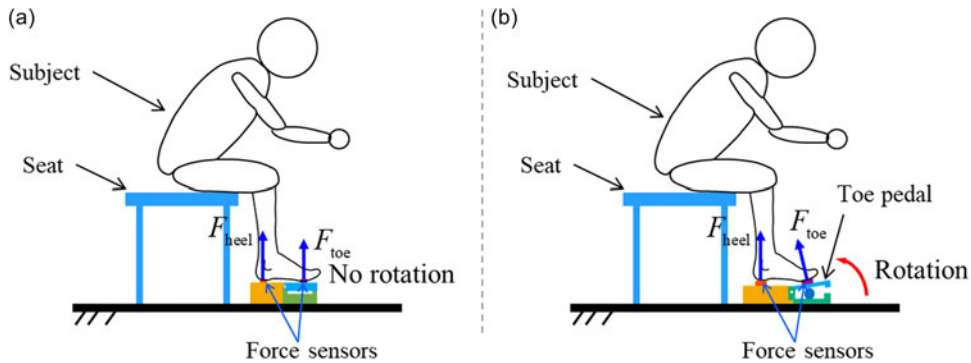
Figure 6. *Comparison of STS-intent detection methods: (a) without stimulus (direct measurement of ground reaction force) and (b) with stimulus (measurement of ground reaction force after mechanical toe stimulus).*
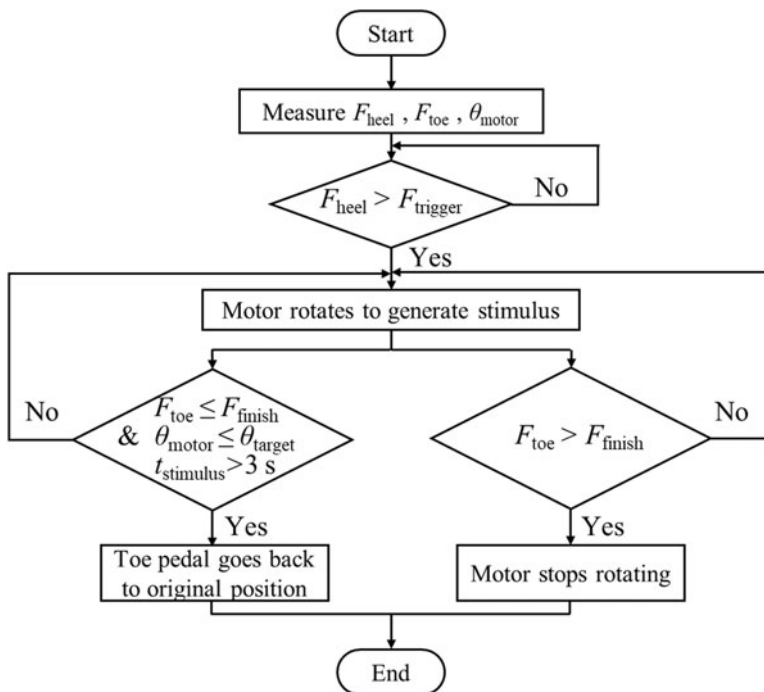

Figure 7. *Flowchart for stimulus application and parameter measurement in STS-intent detection.*

the pedal was activated if F_{heel} exceeded a preset threshold ($F_{trigger}$) because the forward inclination of the trunk caused the center of pressure to shift forward. This transferred more weight onto the heels. Subsequently, the motor rotated to raise the toes and generated a mechanical stimulus. This rotation continued until one of the following two conditions was met: F_{toe} reached the target threshold (F_{finish}), or θ_{motor} reached its maximum limit (θ_{target}). θ_{target} was determined from the ankle dorsiflexion range, which is typically between 0° and 20° [29]. Therefore, the mechanism was designed such that the toe-lifting angle remained within approximately 17°, which is within the safe range of ankle motion. The 17° toe lift corresponds to a motor rotation of approximately 40° owing to the geometry of the four-bar linkage. The motor rotated from 0° to 40° in approximately 0.4 s. To ensure a smooth toe-lifting motion, the control system increases the motor incrementally angle by 1° in every control loop, which is executed at an interval of 10 ms. A fast stimulus is critical for early STS-intent detection. If the toe pedal

rises too slowly, the mechanical stimulus may be delayed, which would reduce the effectiveness of intent detection. In a worst-case scenario, the STS motion might already be completed before the pedal reaches the stimulus angle, hindering timely detection. However, if the motor rotates too quickly, it may cause system instability or discomfort to the user. This speed was confirmed through preliminary trials and was found to be both comfortable for the participants and effective in eliciting measurable toe-reaction forces. F_{finish} was set to approximately 80% of the F_{toe} value observed when the subject finished standing. Therefore, if F_{toe} reaches F_{finish}, it indicates a clear STS intent or that the subject has already stood up. If F_{toe} does not reach the F_{finish} threshold within 3 s ($t_{\text{stimulus}} > 3$ s), it is interpreted as the subject having no intent to stand. The 3 s window was selected based on the experimental setup described in Section 4.3, where a metronome was used to standardize the STS motion duration to 3 s. This duration reflects the typical standing pace of older adults and was consistently applied across all trials to reduce variability [31]. As the participants were instructed to complete the motion in time with the metronome, failing to reach F_{finish} within this period implied either a lack of intent to stand or a delayed reaction inconsistent with the expected STS motion pattern. If the subject intended to stand, they were supposed to complete the STS motion within 3 s, during which F_{toe} would exceed F_{finish}. The toe pedal automatically returned to its initial position to reset the system and prepare for subsequent operations. Throughout the process, both F_{heel} and F_{toe} were continuously measured to detect the STS intent.

3.3. Method for setting thresholds

During the STS process, in addition to analyzing the changes in ground reaction forces (F_{heel} and F_{toe}), the change rate of these forces (ξ_{heel} and ξ_{toe}) was introduced as an additional parameter to enhance the detection rate. This parameter allows the detection of rapid changes in force that are critical during the early phase of the STS motion. To mathematically define these changes, the change rates for the heel reaction force (ξ_{heel}) and toe-reaction force (ξ_{toe}) were calculated as follows:

$$\xi_{\text{heel}} = \frac{F_{\text{heel}(t+\Delta T)} - F_{\text{heel}(t)}}{\Delta T} \tag{1}$$

$$\xi_{toe} = \frac{F_{\text{toe}(t+\Delta T)} - F_{\text{toe}(t)}}{\Delta T} \tag{2}$$

Here, ΔT was set to 40 ms to capture the rapid transitions in the reaction forces during the experiments.

Figure 8 shows a hypothetical graph based on the typical response pattern of a single participant. It does not represent actual experimental data from a specific trial or an average across participants. When the user intends to stand, the ground reaction forces and their rates of change are higher than when there is no intention to stand. Accordingly, the proposed detection method identifies STS intent when the ground reaction forces (F_{heel} and F_{toe}), and their rates of change (ξ_{heel} and ξ_{toe}) simultaneously meet four predefined threshold conditions. If these conditions are not satisfied, the system determines that there is no intention to stand.

1. $F_{heel} \geq F_{heelthre}$
2. $F_{toe} \geq F_{toethre}$
3. $\xi_{heel} \geq \xi_{heelthre}$
4. $\xi_{toe} \geq \xi_{toethre}$

where $F_{heelthre}$, $F_{toethre}$, $\xi_{heelthre}$, and $\xi_{toethre}$ represent the threshold values determined through offline tests.

In Figure 8, t_0 represents the time when the buttocks leave the chair, and t_1 indicates the time when the STS intent is detected. The time difference between these two instants, denoted as Δt in Eq. (3), is a measure of the advance detection time.
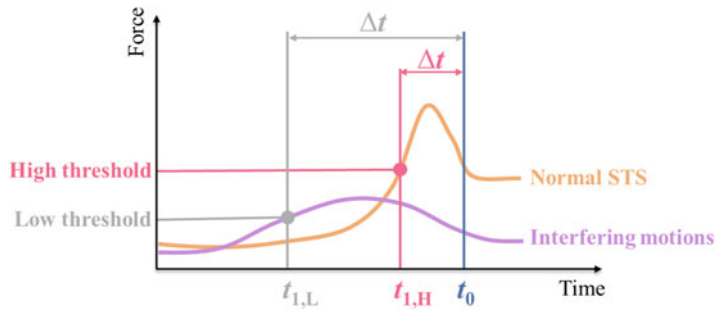
$$\Delta t = t_0 - t_1 \tag{3}$$

Figure 8. *Illustration of the trade-off between the detection rate and advance detection time under different threshold strategies for STS intent.*

The experiment aimed to detect the STS intent before the buttocks left the chair and to effectively distinguish the STS motion from interfering motions. During the threshold section, a trade-off was observed: lower thresholds resulted in a longer advance detection time but a reduced successful detection rate, whereas a higher threshold improved the detection rate at the expense of a shorter advance detection time.

The detection rate was further divided into two metrics:

1. Detection rate of standing up: The percentage of STS motions correctly identified before the buttocks left the chair relative to the total number of STS motions.
2. Detection rate of interfering motions: Percentage of interfering motions correctly identified during the test relative to the total number of interfering motions.

There is a trade-off between the advance detection time and the detection rate. Thus, the Pareto optimization method, which is commonly used in multi-objective optimization [30], was applied to address these conflicting objectives. Section 4.4 introduces the detailed methodology for the threshold selection and data processing.

4. Experiments

4.1. Experimental configuration

This study conducted experiments with five subjects to compare the performance of STS-intent detection with and without a mechanical stimulus, as summarized in Table 1. Each subject performed a normal STS motion and two types of interference motions. In the offline tests, each type of motion was performed five times, and the collected data were analyzed to establish the optimal detection thresholds using the Pareto optimization method. These thresholds were subsequently applied in the online tests, where each motion was repeated 15 times to evaluate the detection rate of standing up, the detection rate of interfering motions, and to advance the detection time (Δt). Finally, the detection performance was assessed by comparing these parameters with and without-stimulus conditions. The STS and interfering motions described in Figs. 5 and 6 were performed by the same five subjects described in Section 4.2.

4.2. Subjects' information

This study serves as a preliminary investigation to evaluate the feasibility of the proposed STS-intent detection method. Initial experiments with young, healthy participants were conducted to establish a foundational understanding of the detection algorithm under controlled conditions. The study group comprised three males and two females, whose information is listed in Table 2. All participants were healthy and capable of performing the STS motion independently. The average body mass index (BMI)

Table I. *Experiment conditions for STS-intent detection: with and without mechanical stimuli.*

Conditions	Motions	STS intent	Number of repetitions
With stimulus	Normal STS	Yes	
	Two types of interfering motions	No	Offline: five times to determine thresholds
Without stimulus	Normal STS	Yes	
	Two types of interfering motions	No	Online: fifteen times to test effectiveness

Table II. *Primary data of the five subjects for testing.*

Code	Age	Weight (kg)	Height (cm)	BMI (kg/m^2)	Gender
Subject #1	23	54	173	18.0	Male
Subject #2	22	59	184	17.4	Male
Subject #3	24	51	162	19.4	Female
Subject #4	26	60	163	22.6	Male
Subject #5	25	60	171	20.5	Female
Average	24.0 ± 1.4	56.8 ± 3.7	170.6 ± 8.0	19.6 ± 1.8	–

of the participants was 19.6 ± 1.8 kg/m^2, indicating that all individuals were within the normal BMI range. Although differences in STS speed may exist between younger and older adults, this study focused on the phase of STS motion before the buttocks left the chair. According to Kojima et al. [31], functionally impaired older adults tend to show greater trunk flexion angles and longer movement durations than young adults. These characteristics may lead to more pronounced changes in ground reaction forces, which could potentially render STS intent easier to detect. Based on these findings, the proposed method shows potential effectiveness in older adults. However, future studies involving older participants are required to validate its feasibility under diverse conditions. The experiments were conducted in accordance with the ethical guidelines established by the Human Subjects Research Ethics Review Committee of the Institute of Science Tokyo (Approval Number: 2022302).

4.3. Offline tests

Each subject performed three types of motions five times per motion during the offline tests. The purpose and structure of the experiment were explained to the subjects. The subjects were instructed to perform the STS motion as naturally as possible without any specific requirements for hand positioning; however, they were explicitly instructed not to use their hands to push against their thighs or the chair during the motion. As shown in Figure 9, the distance between the feet (L), distance from the feet to the chair (B), and distance from the chair seat to the force sensors (H) were adjusted according to the subject's body condition. To make the experiment more reflective of real-life STS motions, the subjects were initially asked to sit in a position that resembled their usual standing posture. Once the position was identified, it was fixed for each subject's main experiment. Previous studies have shown that foot spacing, chair height, and heel-to-chair distance can significantly affect STS performance [32]. Therefore, maintaining consistent L, B, and H distances for each subject throughout the trials ensured uniformity.

Before the test, the subjects were given practice sessions to familiarize themselves with the experimental device. The test began when participants indicated that they were ready. To standardize the motion speed, a metronome was used to set the pace of the STS motion to 3 s to simulate the standing speed of older adults [31]. During each STS motion, F_{heel} and F_{toe} were continuously monitored in real-time, whereas the seat reaction force (F_{seat}) was continuously monitored using a load cell installed on a chair. In the experiments, the stimulus application followed the procedure introduced in Section 3.2. In
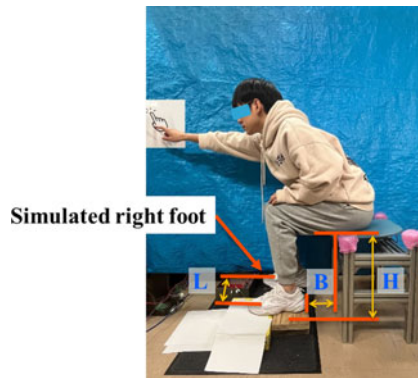
Figure 9. *Relative position of the subject and device in the experimental setup during an offline test.*

contrast, the motor did not rotate during the experiments without a stimulus, and only F_{seat}, F_{heel}, and F_{toe} were measured. The Pareto optimization method established optimal thresholds for detecting STS intent based on data measured during offline testing.

4.4. Data analysis

This section describes the processing of experimental data from offline tests conducted with and without stimuli using the Pareto optimization method. The data analysis procedure is outlined as follows:

Step 1. Reading data

The STS motion data from the five offline experiments, including F_{seat}, F_{heel}, F_{toe}, ξ_{heel}, and ξ_{toe}, and the corresponding time parameters were imported into MATLAB.

Step 2. Normalizing data

• **Normalizing STS time**: Time normalization was applied to ensure consistency across tests. The start of the STS motion (t_{start}) was defined as the instant at which F_{seat} reached its peak. The peak force instant was selected as the starting point because it marks the activation of the hip muscles, which helps move the trunk forward and reduces reaction forces on the feet. Although these muscles create a lifting effect on the thighs, they do not lift the body off the chair but increase F_{seat} as the user begins to stand. The end instant (t_{end}) was defined as the point at which F_{seat} dropped to zero, indicating that the subject's buttocks had left the chair. The duration between t_{start} and t_{end} was calculated using Eq. (4) and served as the basis for time normalization.

$$t_{sum} = t_{end} - t_{start} \tag{4}$$

Each absolute time point (t_{abs}) within this interval was measured relative to t_{start}, resulting in a time difference (t_p), as expressed in Eq. (5). To ensure consistency across different tests, t_p was normalized by dividing it by t_{sum}, as shown in Eq. (6). This normalization scaled the time to a range of 0–1, enabling direct comparisons across tests. As shown in Figure 10, t_{start} and t_{end} are indicated by red circles.

$$t_p = t_{abs} - t_{start} \text{ where } (t_{end} \geq t_{abs} \geq t_{start}) \tag{5}$$

$$t_{norm} = \frac{t_p}{t_{sum}} \tag{6}$$

• **Normalizing reaction forces**: F_{seat}, F_{heel}, and F_{toe} were normalized by dividing each force by the subject's body weight. Figure 10 shows the original reaction forces and their rates of change
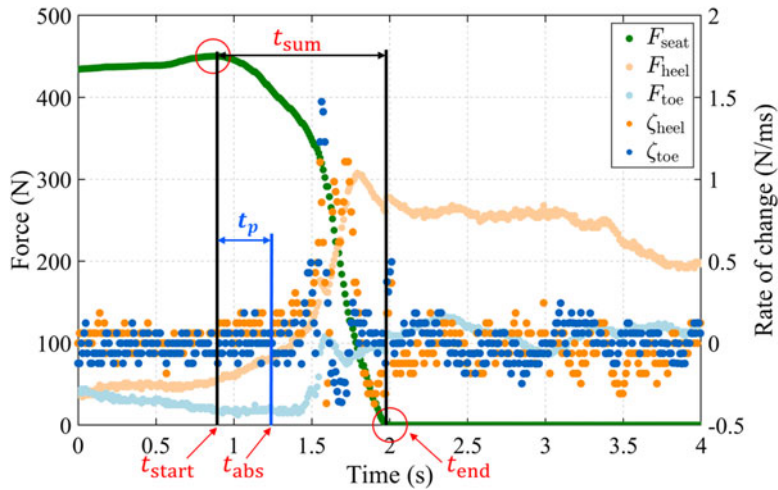
Figure 10. *Example of the reaction force during a single STS motion at the time points used for normalization.*
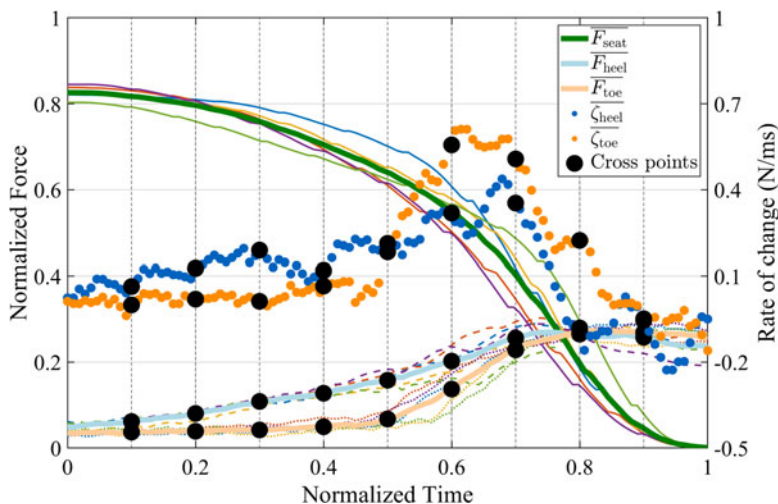

Figure 11. *Normalized reaction forces, corresponding rates of change, and time data for five offline STS motions under stimulus conditions. (The solid lines represent the normalized average force data, and the blue and orange dots indicate the average values of the rate of change of the reaction forces.) The black dots denote the intersection points between the horizontal lines at normalized time intervals from 0.1 to 0.9 and the reaction force or rate-of-change curves. These intersection points collectively form the candidate threshold groups.*

during STS motion, whereas Figure 11 shows the normalized time and reaction force data for five offline STS motions.

Step 3. Generating representative values and constructing threshold combinations
To generate representative thresholds for detecting STS intent, the normalized data from five offline STS motions were first averaged to produce three reference curves: F_{heel}, F_{toe}, and their respective rates of change (ξ_{heel} and ξ_{toe}), as shown in Figure 11. These curves reflect the typical behavior of the ground reaction forces during STS motion and serve as a consistent basis for segmentation. The normalized time

Table III. *Threshold candidate values extracted from nine intervals of normalized time. For each indicator (F_{heel}, F_{toe}, ξ_{heel}, and ξ_{toe}), representative values were sampled at nine time segments ($i = 1$–9), generating 6,561 (9^4) combinations of candidate thresholds.*

Normalized time	$\overline{F}_{\text{heel,i}}$	$\overline{F}_{\text{toe,i}}$	$\overline{\xi}_{\text{heel,i}}$	$\overline{\xi}_{\text{toe,i}}$
0.1	$\overline{F}_{\text{heel,1}}$	$\overline{F}_{\text{toe,1}}$	$\overline{\xi}_{\text{heel,1}}$	$\overline{\xi}_{\text{toe,1}}$
0.2	$\overline{F}_{\text{heel,2}}$	$\overline{F}_{\text{toe,2}}$	$\overline{\xi}_{\text{heel,2}}$	$\overline{\xi}_{\text{toe,2}}$
0.3	$\overline{F}_{\text{heel,3}}$	$\overline{F}_{\text{toe,3}}$	$\overline{\xi}_{\text{heel,3}}$	$\overline{\xi}_{\text{toe,3}}$
0.4	$\overline{F}_{\text{heel,4}}$	$\overline{F}_{\text{toe,4}}$	$\overline{\xi}_{\text{heel,4}}$	$\overline{\xi}_{\text{toe,4}}$
0.5	$\overline{F}_{\text{heel,5}}$	$\overline{F}_{\text{toe,5}}$	$\overline{\xi}_{\text{heel,5}}$	$\overline{\xi}_{\text{toe,5}}$
0.6	$\overline{F}_{\text{heel,6}}$	$\overline{F}_{\text{toe,6}}$	$\overline{\xi}_{\text{heel,6}}$	$\overline{\xi}_{\text{toe,6}}$
0.7	$\overline{F}_{\text{heel,7}}$	$\overline{F}_{\text{toe,7}}$	$\overline{\xi}_{\text{heel,7}}$	$\overline{\xi}_{\text{toe,7}}$
0.8	$\overline{F}_{\text{heel,8}}$	$\overline{F}_{\text{toe,8}}$	$\overline{\xi}_{\text{heel,8}}$	$\overline{\xi}_{\text{toe,8}}$
0.9	$\overline{F}_{\text{heel,9}}$	$\overline{F}_{\text{toe,9}}$	$\overline{\xi}_{\text{heel,9}}$	$\overline{\xi}_{\text{toe,9}}$
Total combinations = $9 \times 9 \times 9 \times 9 = 6{,}561$				

axis was then divided into nine intervals ($i = 1, 2, \ldots, 9$). Four representative values were extracted from the average curves for each interval:

- the mean value of heel force ($\overline{F_{\text{heel,i}}}$);
- mean value of toe force ($\overline{F_{\text{toe,i}}}$);
- mean value of heel force rate of change ($\overline{\xi_{\text{heel,i}}}$); and
- mean value of toe-force rate of change ($\overline{\xi_{\text{toe,i}}}$).

As shown in Table 3, this process resulted in nine candidate values for each indicator, and by selecting one value from each of the four, a total of 6,561 (9^4) unique combinations of threshold candidates were generated.

Step 4. Testing threshold combinations
Each of the 6,561 candidate threshold combinations was applied to the offline dataset to evaluate detection performance. STS intent is considered detected only when all four threshold conditions are simultaneously satisfied. The advance detection time (Δt) and detection rate of the interfering motions for each combination were then computed. As shown in Figure 12, t_1 denotes the first detected STS-intent timing, and the advance time Δt was calculated using Eq. (3).

Step 5. Filtering invalid combinations
Threshold combinations resulting in $\Delta t \leq 0$ were excluded from consideration, as they failed to detect the user's STS intent before the buttocks left the chair. As early detection is critical for providing timely assistance in AAN-based systems, these threshold groups were considered ineffective for practical use and removed from further analysis. This filtering step ensures that the final selected thresholds guarantee accuracy and timely detection.

Step 6. Plotting the Pareto front
To construct the Pareto optimization, the detection rates of the interfering motions were plotted along the horizontal axis. Cases where $\Delta t > 0$ were plotted on the vertical axis, as shown in Figure 13. The resulting Pareto front illustrated the trade-off between the detection rate and Δt, which helped identify the optimal thresholds. Points 1–4 were selected along the Pareto front, representing different trade-offs.
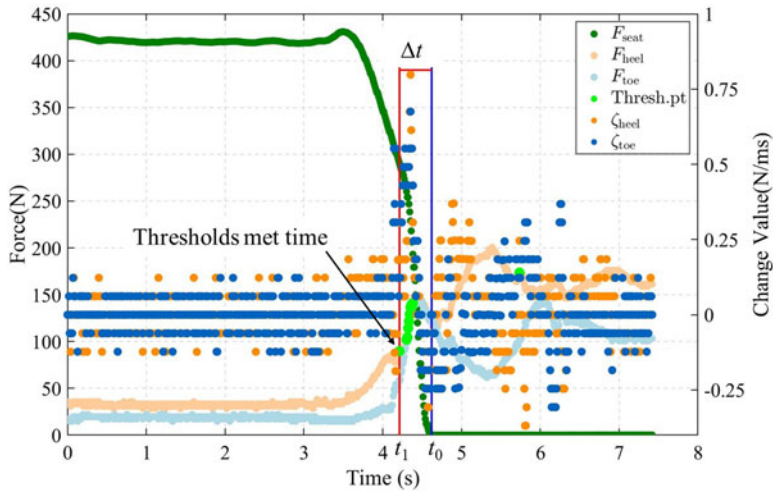
Figure 12. *Example of applying set thresholds to detect STS intent during an STS motion test. The green dots indicate the time points that meet the conditions defined by the thresholds.*
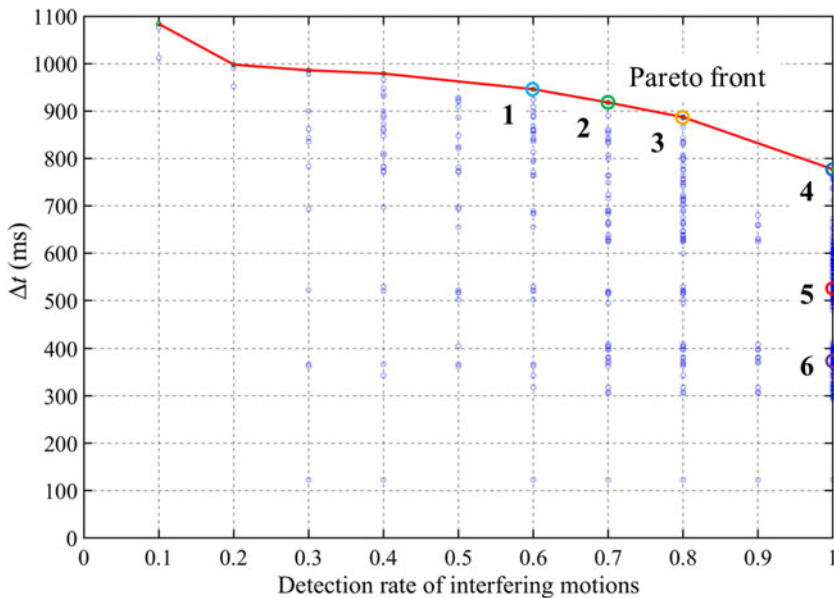

Figure 13. *Experimental data processing results using Pareto optimization. The Pareto front is shown for different threshold candidates with stimulus.*

For example, Point 1 emphasizes early detection (larger Δt) at the cost of a lower detection rate, whereas Point 4 maintains a higher accuracy with a moderately reduced advance time. In addition, Points 5 and 6, although not on the Pareto front, were deliberately selected as high-threshold cases with a detection rate of 1 to evaluate the detection robustness under stricter conditions. These points correspond to more conservative threshold settings with small Δt values. Each selected point corresponded to a unique combination of the four thresholds. The proposed method detects STS intent only when all four conditions are simultaneously satisfied: the ground reaction forces (F_{heel} and F_{toe}) and their rates of change (ξ_{heel} and ξ_{toe}) must exceed their respective thresholds. If any condition is not met, the system determines that there is no intent to stand. Finally, these six points were applied to the online tests to
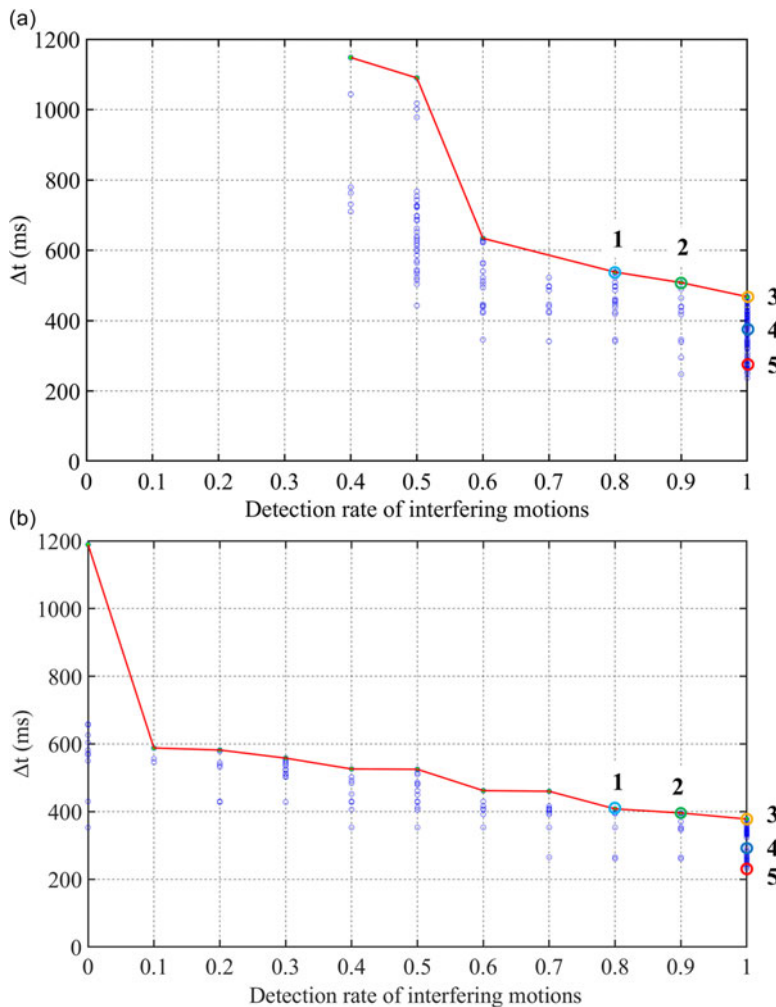
Figure 14. *Example of experimental data processing results using Pareto optimization with and without stimuli. (a) Pareto optimization of Subject #1 with stimulus. (b) Pareto optimization of Subject #1 without stimulus.*

evaluate whether similar detection behavior could be observed under real-time conditions. The consistency between the offline and online results supports the use of offline-optimized thresholds in practical applications.

4.5. Online tests

Figure 14 shows the Pareto optimization plot for Subject #1 with and without stimulus. Points 1–5, including the Pareto front (1–3) and additional points with a detection rate of 1 (Points 4 and 5), were selected and applied to online tests to evaluate their detection rates and Δt. The online testing process was the same as the offline tests, except that the predetermined threshold values were integrated into the detection program for real-time STS-intent detection. The results were compared between the conditions with and without stimuli. The same procedure was repeated for all the other subjects. The specific threshold parameters used for each point (Points 1–5) under both conditions are listed in Table 4.

Table IV. *Threshold parameter settings and corresponding detection rates for Points 1–5 on the Pareto front shown in Figure 14, under conditions with and without stimuli.*

Conditions	Points	F_{heelthr} (N)	F_{toethr} (N)	ξ_{heelthr} (N/ms)	ξ_{toethr} (N/ms)	Detection rate of interfering motions
With stimulus	1	85.27	20.06	0.19	0.07	0.8
	2	85.27	20.06	0.19	0.18	0.9
	3	33.36	20.06	0.32	0.01	1
	4	33.36	74.16	0.32	0.56	1
	5	139.26	20.06	0.06	0.01	1
Without stimulus	1	27.7	17.93	0.18	0.11	0.8
	2	27.7	33.85	0.18	0.11	0.9
	3	27.7	17.93	0.18	0.18	1
	4	82.92	17.93	0.27	0.27	1
	5	141.59	75.2	0.27	0.00	1

5. Results

5.1. Comparison of force characteristics during different motions with and without stimuli for Subject #1

Figure 15 presents a comparative example of the online test results for the three types of motion performed by Subject #1. The results indicate that the F_{heel}, F_{toe}, ξ_{heel}, and ξ_{toe} values are significantly higher for the STS motion (Figure 15(a) and (b)) than for the two types of interfering motions (Figure 15(c), (d), (e), and (f)). The STS intent can be correctly detected by setting the optimal thresholds using the Pareto optimization method. Figure 15(a) and (b) show the STS motion with and without stimuli, respectively. The advance time Δt was calculated using Eq. (3). A comparison of Figure 15(a) and (b) reveals that when the toe pedal is lifted and the subject intends to stand, F_{toe} increases sharply. In contrast, under the without-stimulus condition, F_{toe} increased more gradually, with the primary reaction force focused on F_{heel}. This study leveraged the sharp increase in F_{toe} triggered by the toe pedal to improve the detection rate and stability of STS intent. Instances in which the motor angle appears as a negative value result from a slight deformation of the toe pedal under a high force, causing a brief reverse rotation of the encoder and producing negative readings.

The interfering motions are illustrated in Figure 15(c), (d), (e), and (f).

1) *Change in F_{toe}*: Under the stimulus condition, F_{toe} increased significantly after the toe pedal was lifted, as illustrated in Figure 15(c) and (e). This result highlights the influence of the stimulus on toe-force generation.

2) *Change in F_{heel}*: The behavior of F_{heel} varied depending on the presence of stimuli. In the absence of a stimulus, F_{heel} increased during the interfering motions, as shown in Figure 15(d) and (f). However, with the applied stimulus, F_{heel} decreased, as shown in Figure 15(c). Furthermore, in Figure 15(e), the rate of increase in F_{heel} is lower than that in Figure 15(f), indicating a moderating effect of the stimulus on the heel reaction force dynamics.

These changes in the ground reaction forces under stimulus conditions, as shown in Figure 15, make it more difficult to satisfy the thresholds for detecting the STS intent during interfering motions, thereby increasing the detection rate of interfering motions.

In addition to the qualitative observations described above, a detailed statistical analysis was conducted to quantitatively validate the variations in the force characteristics across different motions and conditions. Figure 16 presents a comparison of the average maximum values of F_{heel}, F_{toe}, ξ_{heel}, and ξ_{toe} across 15 trials during the normal STS, forward, and pick-up motions without a stimulus. For the STS motion, the maximum values were extracted before the buttocks left the chair, as our intention-detection
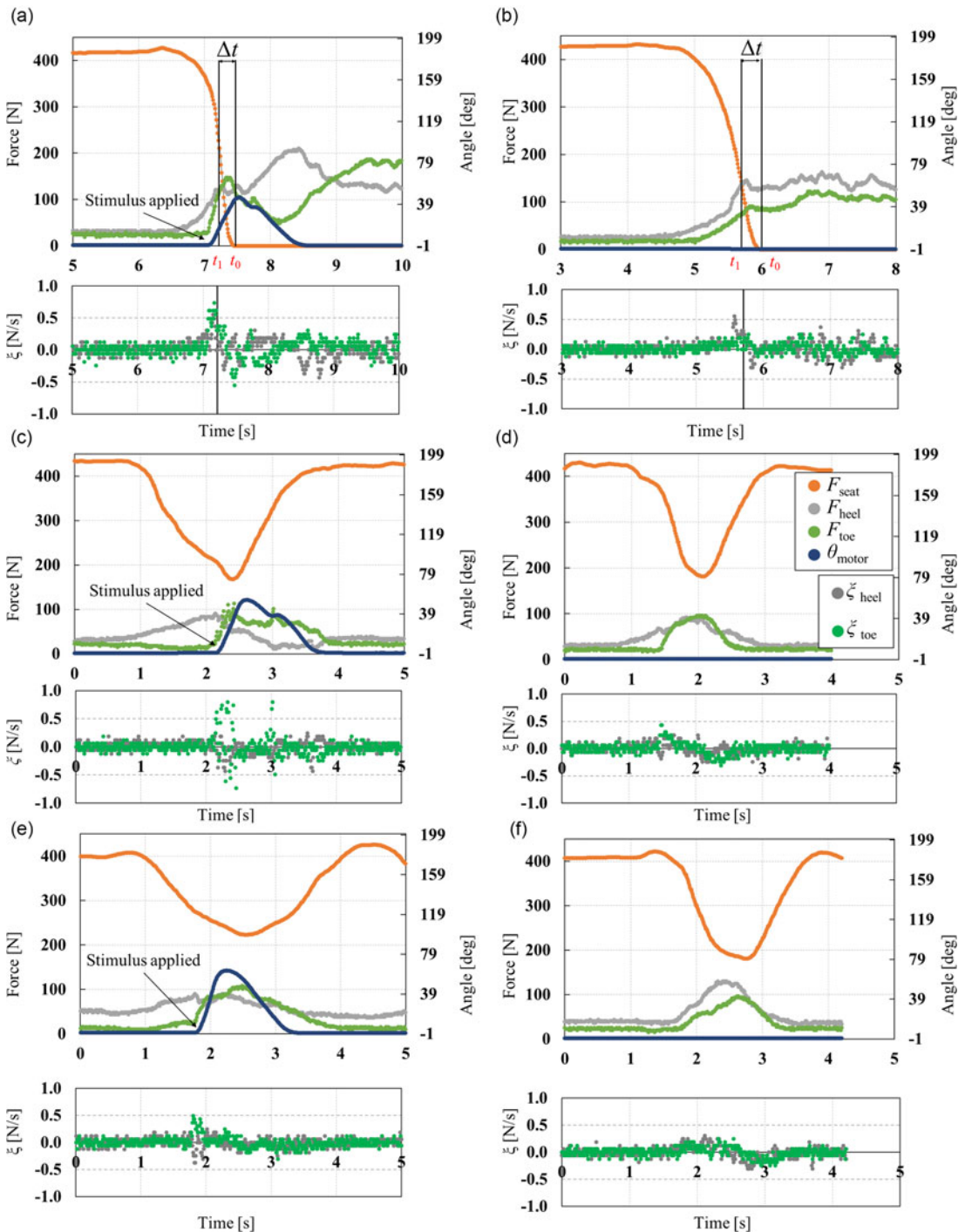
Figure 15. *Example figure comparing the online test results for the three types of motions performed by Subject #1. The figure shows the time-based changes in F_{heel}, F_{toe}, ξ_{heel}, ξ_{toe}, θ_{motor} (with the initial rotation indicating when the toe pedal began to rotate), and F_{seat}. (a) (b) Normal STS motion with and without a stimulus. (c) (d) Grabbing items in front with and without a stimulus. (e) (f) Picking up an item from the ground with and without a stimulus.*
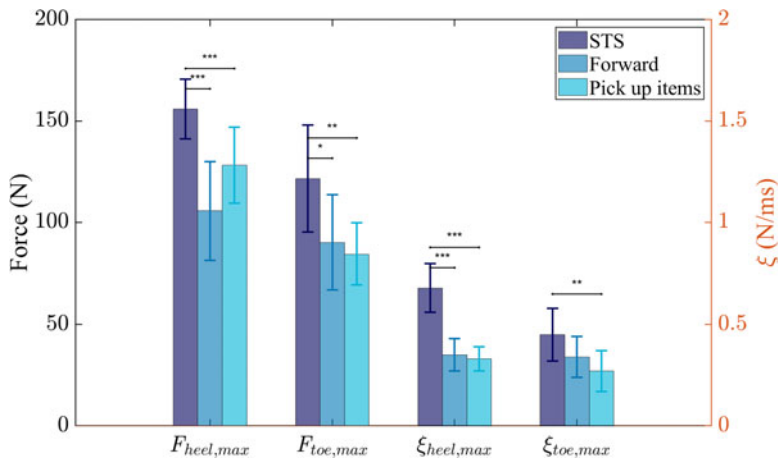
Figure 16. *Comparison of maximum F_{heel}, F_{toe}, ξ_{heel}, and ξ_{toe} of Subject #1 during STS, forward, and pick-up motions without stimulus. Statistical significance is indicated as follows: *$p < 0.05$, **$p < 0.01$, ***$p < 0.001$.*
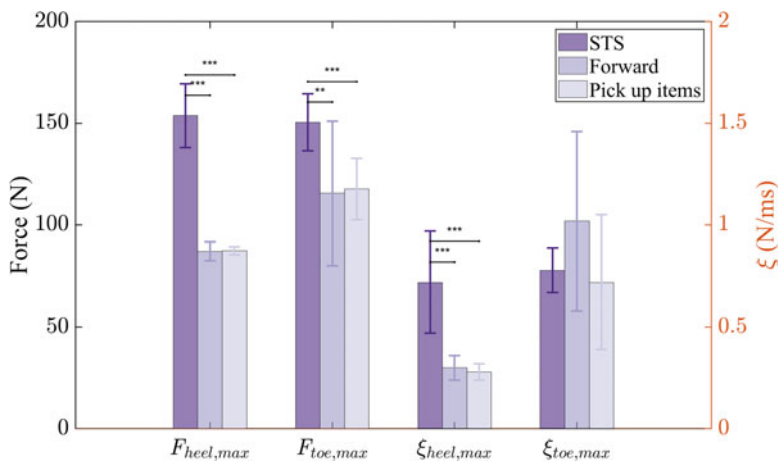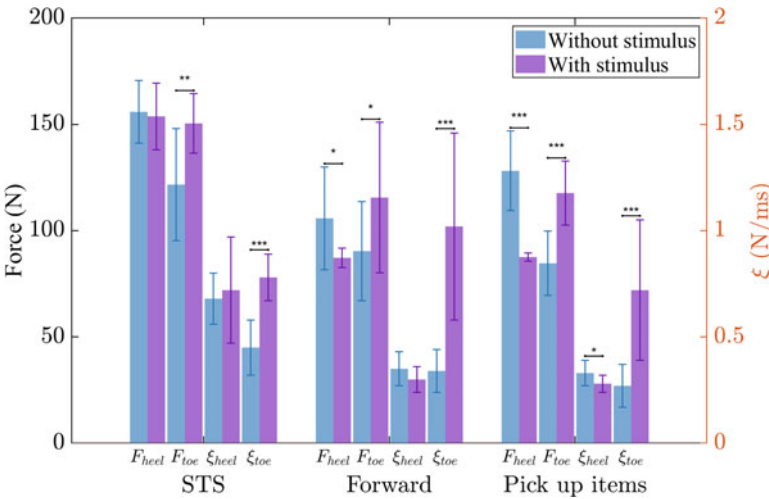

Figure 17. *Comparison of maximum F_{heel}, F_{toe}, ξ_{heel}, and ξ_{toe} of Subject #1 during STS, forward, and pick-up motions under the stimulus condition. Statistical significance is indicated as follows: *$p < 0.05$, **$p < 0.01$, ***$p < 0.001$.*

model aims to predict the standing intention during this critical pre-seat-off phase. Statistical analyses (paired two-tailed t-tests) revealed that during this phase, the maximum values of all four parameters during normal STS motion were significantly higher than those during the interfering motions (forward and pick-up motions), indicating clear mechanical differences associated with the standing intention. In addition, the results showed that the F_{heel} values were greater than the F_{toe} values during the normal STS motion, suggesting that the participants relied more on their heels during the standing process.

Figure 17 shows the corresponding comparison under the stimulus condition. Owing to the application of toe-pedal stimulation, the participant's response caused a rapid increase in both F_{toe} and ξ_{toe} during the intention-detection phase. This externally induced toe response provided a clearer and more reliable basis for detecting STS intention. Figure 18 compares the results between the conditions with and without stimuli. Toe pedal stimulation not only led to significant increases in F_{toe} and ξ_{toe}, but also resulted in decreases in F_{heel} and ξ_{heel} during the interfering motions. This simultaneous increase in F_{toe}/ξ_{toe} and decrease in F_{heel}/ξ_{heel} resulted in a more distinct separation between the parameters under

Table V. *Online tests with stimulus results in Figure 14(a).*

No. of selected points	1	2	3	4	5	Variation tendency
Coordinate (offline)	(0.8,408)	(0.9,396)	(1.0,378)	(1.0,329)	(1.0,245)	–
Advance detection time Δt (ms)	386	369	362	316	277	Δt decrease
Offline and online Δt difference (ms)	22	27	16	13	**32**	–
Detection rate of STS motion	100%	100%	100%	93%	80%	Rate decrease
Detection rate of interfering motions	80%	80%	93%	100%	100%	Rate increase

Figure 18. *Comparison of maximum F_{heel}, F_{toe}, ξ_{heel}, and ξ_{toe} of Subject #1 during STS, forward, and pick-up motions under conditions with and without stimulus. Statistical significance is indicated as follows: $^*p < 0.05$, $^{**}p < 0.01$, $^{***}p < 0.001$.*

the stimulus condition, thereby enhancing the robustness of the intention-detection algorithm when the four threshold conditions were simultaneously satisfied.

In summary, the statistical analysis confirmed significant variations in the parameters across different motions and conditions and demonstrated the effectiveness of toe-pedal stimulation in improving the accuracy and robustness of standing intention detection. It should be noted that the maximum values analyzed did not necessarily occur simultaneously. Therefore, the detection of the standing intention was not based on a single instantaneous value but on the simultaneous satisfaction of all four threshold conditions, ensuring higher reliability.

5.2. Comparison of detection rate and advance time with and without stimuli for Subject #1
The threshold values corresponding to the selected Points (1–5) for Subject #1 in Figure 14 are listed in Table 4. These threshold values were applied to the online tests, and the results are presented in Tables 5 and 6. These tables summarize the performance of the system in detecting STS intent with and without stimuli.

Table VI. *Online tests without stimulus results in Figure 14(b).*

No. of selected points	1	2	3	4	5	Variation tendency
Coordinate (offline)	(0.8,528)	(0.9,508)	(1.0,468)	(1.0,361)	(1.0,278)	–
Advance detection time Δt (ms)	535	509	487	370	288	Δt decrease
Offline and online Δt difference (ms)	7	1	19	9	10	–
Detection rate of STS motion	100%	100%	100%	80%	60%	Rate decrease
Detection rate of interfering motions	20%	20%	40%	97%	100%	Rate increase

1) *Detection Rate of STS Motion*: The detection rate of STS motion under the stimulus condition remained consistently high at approximately 100% across most thresholds. Slight reductions were observed at Points 4 (93%) and 5 (80%), demonstrating the capability of the system to reliably detect STS intent when a stimulus was applied. In contrast, under the without-stimulus condition, the detection rate exhibited greater variability. At higher thresholds (Points 4 and 5), the detection rate decreased significantly, with Point 5 reaching 60%.

2) *Detection Rate of Interfering Motions*: For interfering motions, the stimulus condition achieved high detection rates, reaching 100% at higher thresholds (Points 4 and 5). This highlights the ability of the system to effectively differentiate STS motions from other interfering motions. However, in the without-stimulus condition, the detection rates were less reliable, with values below 40% at Points 1, 2, and 3. Although Points 4 and 5 showed improvement, this was at the expense of the detection rate for STS motion.

3) *Advance Detection Time (Δt)*: The advance detection time (Δt) from online tests was closely aligned with that from offline tests in both conditions, with differences of less than 32 ms. This consistency underscores the reliability of the thresholds established during offline tests for real-time applications. Additionally, as the thresholds increased, Δt decreased, reflecting a trade-off between early detection and detection accuracy.

4) *Performance Comparison*: The stimulus condition outperformed the without-stimulus condition in balancing early detection and accurate differentiation. Under the stimulus condition, high detection rates for both STS and interfering motions were achieved while maintaining the stability of the detection system across the thresholds. In contrast, the without-stimulus condition struggled to achieve this balance, leading to lower detection rates and greater variability.

5.3. Comparison of detection results across all subjects with and without stimuli

To validate the effectiveness of the proposed method, STS and interfering motions corresponding to selected points on the Pareto optimization plot were applied to the online tests. Specifically, thresholds corresponding to points on the Pareto front were selected where the detection rate of the interfering motions reached 100% (e.g., Point 3 – yellow circle in Figure 14). Figure 19 presents the results of these online tests across five subjects (S1–S5). In Figure 19(a), the average advance detection time (Δt) for the "with stimulus" and "without stimulus" conditions is compared for five subjects. The results indicate that, although S3–S5 exhibited earlier detection under the stimulus condition, this trend was not consistent for all participants. Moreover, S1 and S2 showed shorter advance times in the without-stimulus condition. Furthermore, statistical analysis revealed that only two subjects exhibited significant differences between the two conditions. These results suggest that the stimulus does not consistently benefit detection timing.
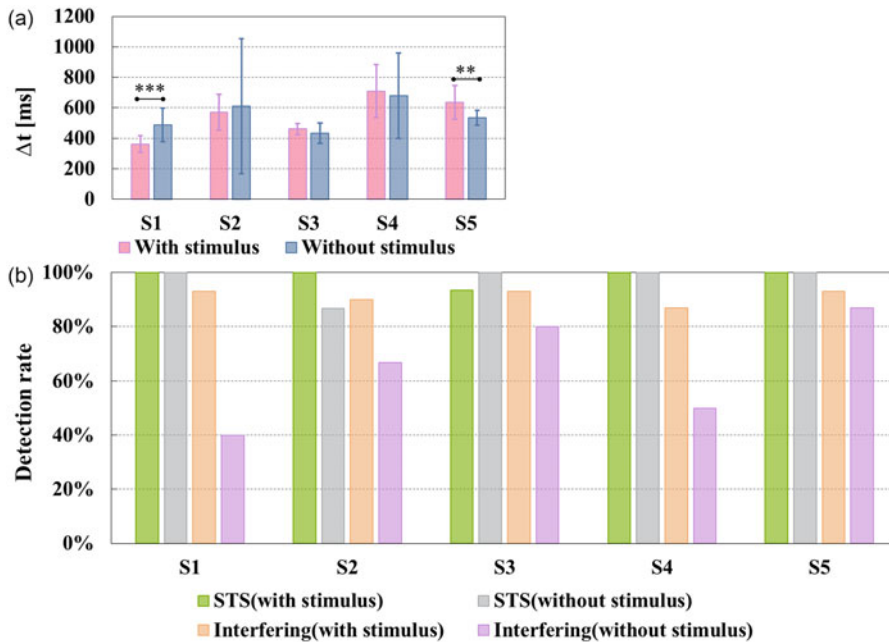
Figure 19. *Online test results under conditions with and without stimulus for five subjects (S1–S5 denote Subject #1 through to Subject #5), using thresholds from points on the Pareto front where the detection rate of interfering motions is equal to 1. (a). Advance detection time Δt (b). Detection rates of STS motion and interfering motions under both conditions. Statistical significance is indicated as follows:**$p < 0.01$, ***$p < 0.001$.*

In contrast, Figure 19(b) highlights the advantages of the stimulus condition in terms of detection robustness. Specifically, although both conditions achieved high detection rates for STS motion, the detection rates for the interfering motions were significantly higher under the stimulus condition across all subjects. This indicates that the application of a toe-pedal stimulus improves the robustness and reliability of the system in distinguishing true standing intentions from interfering motions.

6. Discussion

6.1. Effectiveness and advantages of external mechanical stimulus in STS-intent detection

This study proposed a method for detecting STS intent by applying an external mechanical stimulus, demonstrating a higher detection rate of STS motion and more consistent detection of interfering motions than without stimulus. During the STS process, most of the body weight is concentrated on the heels. However, in the early stages of standing, lifting the toes shifted part of the weight forward, rapidly increasing F_{toe} and F_{heel}. This shift in force can facilitate a more accurate and earlier detection of STS intent, a process that can be potentially enhanced by external mechanical stimuli. The physiological mechanism by which a mechanical stimulus affects the user's response remains unclear and requires further exploration. Further studies involving detailed biomechanical and neuromuscular analyses are necessary to better understand user responses to mechanical stimuli during STS motion. Nevertheless, the current findings suggest that applying such stimuli holds promise for enhancing the accuracy and reliability of STS-intent detection systems.

The AAN STS device is designed to encourage users to use their muscles to stand while providing timely assistance only when necessary. Accurate and early detection of STS intent is essential for such devices because it allows sufficient time for the system to respond to user needs and deliver prompt support. This timely intervention can help prevent situations in which the user may struggle to stand

or, in severe cases, risk falling owing to a loss of balance. Although this study proposes a detection method and evaluates its performance, it has not yet been applied to practical STS-assistive devices. To bridge the gap between research and practical applications, this method should be integrated into actual assistive devices to ensure seamless implementation and enhance effectiveness and usability.

Compared with existing wearable-based STS intention estimation methods, such as those proposed by Li et al. [14] and Hiyama et al. [16], our approach demonstrates clear advantages in terms of system simplicity, earlier response timing, and user convenience. Li et al.'s method relies on a combination of EMG sensor and trunk angle data obtained via a smartphone, and intention detection is triggered only when both indicators exceed predefined thresholds. Although this approach has relatively robust logic, it requires the user to wear EMG sensors and to fix a smartphone to the body, which introduces operational burdens, particularly for elderly users. Moreover, although their study claims to detect intention during the early phase of the STS process (such as immediately after the buttocks leave the chair), the decision logic also incorporates information from the period after the buttocks leave the chair, and no clear trigger timing or lead time is quantitatively reported. Their conclusions are supported only by slow-motion experimental analysis, making comparisons difficult because of the lack of quantified time references. In contrast, Hiyama et al. proposed a method that used EMG sensors and a 9-axis IMU sensor. By analyzing the increasing trend of trunk angle data and the sequential activation of lower-limb muscles, their system predicted STS intention with an average lead time of 97.3 ms before the buttocks left the chair, achieving a detection accuracy of 99.5%, demonstrating high sensitivity and reliability. Although the authors did not specify the total duration of the STS motion, the experimental results shown in their figure suggest that a complete STS cycle lasts approximately 3 s, which is consistent with the average duration observed in our study.

In comparison, our method for detecting STS intent using a mechanical stimulus to the toes and analyzing the resulting ground reaction force does not require any wearable sensors. Experimental results show that our system can detect STS intent approximately 400 ms before the buttocks leave the chair, which is earlier than the above method. Although the detection accuracy of our method is slightly lower, at approximately 90%, its advantages in terms of lead time, non-invasiveness, and system simplicity make it particularly suitable for practical use, particularly for users who may be sensitive to, or have difficulty with, wearable devices.

6.2. Limitations and future work

This study had some limitations that must be addressed in future studies. First, the feasibility and effectiveness of the method were tested only in young, healthy subjects. Improvements in device safety and convenience are necessary to evaluate its practicality and broaden its scope of applications. Future experiments should include older adults and individuals with mobility impairments to assess the effectiveness of this method in a broader population. In addition, individuals with difficulty standing often use supportive objects, such as handrails, to assist them. The current study did not consider the conditions involving the use of this support. Handrails can redistribute the weight of the upper body, leading to decreased ground reaction forces, which could affect the early and accurate detection of STS intent and the ability to distinguish it from other interfering motions. To address this problem, initial offline experiments will be conducted using handrails to establish appropriate thresholds based on the measured plantar reaction force data. The proposed method was applied under these conditions to evaluate its performance in detecting STS intent. Suppose the method proves insufficient for providing accurate and quick detection. In this case, the incorporation of additional force sensors on the handrails or other supports should be considered to develop a new approach that accounts for the forces exerted between the hands and supports.

This approach demonstrates the potential for integration into future STS-assistive devices. By achieving a high detection rate and robust stability in detecting the STS intent, these devices can provide timely support, allowing users to utilize their strengths to stand while ensuring safety. Future studies will involve

integrating this method into an assistive device to evaluate its performance and effectiveness in practical applications.

7. Conclusion

This study presents a novel method for detecting STS intent by applying a mechanical stimulus to the toes and relying solely on the resulting heel and toe-reaction forces. A method that maintains a high detection rate and early detection time, while lowering the complexity of the sensor system, was developed by analyzing the reaction forces and their variations after a toe stimulus. This method demonstrated a high detection rate for STS intent in healthy subjects. In addition, the Pareto optimization method was effectively employed to automate the threshold-setting process, allowing customization according to individual user needs. The comparison between conditions with and without stimuli indicated that the stimulated condition resulted in more accurate and stable detection of STS intent. This detection method is promising for integration into AAN STS-assistive devices.

References

[1] M. A. Hughes, "Chair rise strategy in the functionally impaired elderly," *J. Rehabil. Res. Dev.* **33**(4), 409–412 (1996).

[2] M. M. Gross, P. J. Stevenson, S. L. Charette, G. Pyka and R. Marcus, "Effect of muscle strength and movement speed on the biomechanics of rising from a chair in healthy elderly and young women," *Gait Posture* **8**(3), 175–185 (1998). doi: 10.1016/S0966-6362(98)00033-2.

[3] A. Tsukahara, R. Kawanishi, Y. Hasegawa and Y. Sankai, "Sit-to-stand and stand-to-sit transfer support for complete paraplegic patients with robot suit HAL," *Adv. Robot.* **24**(11), 1615–1638 (2010). doi: 10.1163/016918610X512622.

[4] S. Sugiura, J. Unde, Y. Zhu and Y. Hasegawa, "Variable grounding flexible limb tracking center of gravity for sit-to-stand transfer assistance," *IEEE Robot. Autom. Lett,* **9**(1), 175–182 (2024). doi: 10.1109/lra.2023.3328449.

[5] B. Chen, C.-H. Zhong, H. Ma, X. Guan, L.-Y. Qin, K.-M. Chan, S.-W. Law, L. Qin and W.-H. Liao, "Sit-to-stand and stand-to-sit assistance for paraplegic patients with CUHK-EXO exoskeleton," *Robotica* **36**(4), 535–551 (2018). doi: 10.1017/S0263574717000546.

[6] T. Wang, Y. Wang, J. Yang and S. Wang. "Study on Assistance Force of Standing Assist Robot." **In:** *2021 IEEE International Conference on Intelligence and Safety for Robotics (ISR)*, Tokoname, Japan: IEEE (2021) pp. 373–377. doi: 10.1109/ISR50024.2021.9419518.

[7] D. Chugo, S. Muramatsu, S. Yokota, J.-H. She and H. Hashimoto, "Stand-up assistive devices allowing patients to perform voluntary movements within the safety movement tolerance," *J. Artif. Intell. Technol.* **2**(4), 164–173 (2022). doi: 10.37965/jait.2022.0121.

[8] N. Naghavi, A. Akbarzadeh, S. M. Tahamipour-Z. and I. Kardan, "Assist-As-Needed control of a hip exoskeleton based on a novel strength index," *Robot. Auton. Syst.* **134**, 103667 (2020). doi: 10.1016/j.robot.2020.103667.

[9] J. L. O'Loughlin, Y. Robitaille, J.-F. Boivin and S. Suissa, "Incidence of and risk factors for falls and injurious falls among the community-dwelling elderly," *Am. J. Epidemiol.* **137**(3), 342–354 (1993).

[10] M. K. Shepherd and E. J. Rouse. "Design and Characterization of a Torque-controllable Actuator for Knee Assistance During Sit-to-Stand." **In:** *2016 38th Annual International Conference of the IEEE Engineering in Medicine and Biology Society (EMBC)*, Orlando, FL, USA: IEEE (2016) pp. 2228–2231. doi: 10.1109/EMBC.2016.7591172.

[11] H. Jeong, A. Guo, T. Wang, M. Jun and Y. Ohno. "Development of Four-Bar Linkage Mechanism on Chair System for Assisting Sit-to-Stand Movement." **In:** *2019 IEEE 4th International Conference on Advanced Robotics and Mechatronics (ICARM)*, Toyonaka, Japan: IEEE (2019) pp. 303–308. doi: 10.1109/ICARM.2019.8833922.

[12] R. Lizama-Pérez, L. J. Chirosa-Ríos, G. Contreras-Díaz, D. Jerez-Mayorga, D. Jiménez-Lupión and I. J. Chirosa-Ríos, "Effect of sit-to-stand-based training on muscle quality in sedentary adults: A randomized controlled trial," *PeerJ* **11**, e15665 (2023).

[13] Ministry of Health, Labour and Welfare of Japan. *Classification of Certification for Long-term Care* (Ministry of Health, Labour and Welfare of Japan, Tokyo, 2023). Available: https://www.mhlw.go.jp/topics/kaigo/kentou/15kourei/sankou3.html.

[14] B. Li, H. B. A. Qiong Gui, H. Li and Z. Jin. "A Wearable Sit-to-Stand Detection System Based on Angle Tracking and Lower Limb EMG." **In:** *2016 IEEE Signal Processing in Medicine and Biology Symposium (SPMB)*, Philadelphia, PA, USA: IEEE (2016) pp. 1–6. doi: 10.1109/SPMB.2016.7846876.

[15] T. Inoue and R. Matsuo. "Prediction of Sit-to-Stand Time Using Trunk Angle and Lower Limb EMG for Assistance System." **In:** *2020 IEEE 2nd International Conference on Artificial Intelligence in Engineering and Technology (IICAIET)*, Kota Kinabalu, Malaysia: IEEE (2020) pp. 1–4. doi: 10.1109/IICAIET49801.2020.9257818.

[16] T. Hiyama, Y. Kato and T. Inoue. "Sit-to-Stand Assistance System Based on Using EMG to Predict Movement." **In:** *2017 26th IEEE International Symposium on Robot and Human Interactive Communication (RO-MAN)*, Lisbon: IEEE (2017) pp. 81–87. doi: 10.1109/ROMAN.2017.8172284

[17] W. Yuan, K. Zou, Y. Zhao and N. Xi. "Detection of Human Action Intention by Electromyography (EMG)." **In:** *2022 12th International Conference on CYBER Technology in Automation, Control, and Intelligent Systems (CYBER)*, Baishan, China: IEEE (2022) pp. 750–754. doi: 10.1109/CYBER55403.2022.9907225.

[18] A. J. Young, T. A. Kuiken and L. J. Hargrove, "Analysis of using EMG and mechanical sensors to enhance intent recognition in powered lower limb prostheses," *J. Neural Eng.* **11**(5), 056021 (2014). doi: 10.1088/1741-2560/11/5/056021.

[19] A. Arcelus, I. Veledar, R. Goubran, F. Knoefel, H. Sveistrup and M. Bilodeau, "Measurements of sit-to-stand timing and symmetry from bed pressure sensors," *IEEE Trans. Instrum. Meas.* **60**(5), 1732–1740 (2011). doi: 10.1109/TIM.2010.2089171.

[20] A. Arcelus, R. Goubran, F. Knoefel, H. Sveistrup and M. Bilodeau. "Detection of Bouncing During Sit-to-Stand Transfers with Sequential Pressure Images." **In:** *2011 IEEE International Symposium on Medical Measurements and Applications*, Bari, Italy: IEEE (2011) pp. 158–161. doi: 10.1109/MeMeA.2011.5966665.

[21] E. Cao, Y. Inoue, T. Liu and K. Shibata, "A sit-to-stand training robot and its performance evaluation: Dynamic analysis in lower limb rehabilitation activities," *JSDD* **6**(4), 466–481 (2012). doi: 10.1299/jsdd.6.466.

[22] Y. Tsusaka, F. Dallalibera, Y. Okazaki, M. Yamamoto and Y. Yokokohji, "Development of a standing-up motion assist robot considering physiotherapist skills that bring out abilities from the patient," *Trans. JSME (in Japanese)* **83**(852), 17-00058–17-00058 (2017). doi: 10.1299/transjsme.17-00058.

[23] J. Bell and H. H. Asada. "Monitoring the Mental State of Cooperativeness for Guiding an Elderly Person in Sit-to-Stand Assistance." **In:** *2022 International Conference on Robotics and Automation (ICRA)*, Philadelphia, PA, USA: IEEE (2022) pp. 6465–6471. doi: 10.1109/ICRA46639.2022.9812422.

[24] Y. Egahara and S. Yamamoto. *Introduction to Body Dynamics: Analysis of the Sit-to-Stand Movement (in Japanese)* (Ishiyaku Publishers, Inc, Tokyo, 2018).

[25] J. Zheng, M. Jiang, A. Botta, Y. Sugahara and Y. Takeda. Detection of Intent in Sit-to-Stand Using Plantar Reaction Force in Response to External Stimulus On Toe (In Japanese). **In:** *LIFE2023* (2023) p. 3A1E3.

[26] M. Jiang, J. Zheng, A. Botta, Y. Sugahara and Y. Takeda, "Estimation of Sit-to-Stand Intentions via Plantar Force Reaction Induced by External Stimulus on Toe," **In:** *29th Robotics Symposia*, Japan (2024).

[27] M. Jiang, J. Zheng, Q. Meng, Y. Sugahara and Y. Takeda. "Detecting the Intention of Sit-to-Stand by Analyzing Reaction Forces on the Foot with Pareto Optimum." **In:** *2024 46th Annual International Conference of the IEEE Engineering in Medicine and Biology Society (EMBC)*, Orlando, FL, USA: IEEE (2024) pp. 1–4. doi: 10.1109/EMBC53108.2024.10782011.

[28] Zozo Corporation. *Zozo Corporation Report* (Zozo Corporation, Chiba, Japan, 2020). Available: https://corp.zozo.com/assets_wp/cf/ja/wp-content/uploads/2020/06/05f3c91e68fda8153a6aa9f5111d7cc7.pdf.

[29] Japanese Journal of Rehabilitation Medicine, "Revision of the standard for joint range of motion presentation and measurement methods (April 2022 revision)." *Jpn. J. Rehabil. Med.* **58**(10), 1188–1200 (2022). doi: 10.2490/jjrmc.58.1188.

[30] J. S. Arora. *Introduction to Optimum Design*. 3rd edition (Academic Press, Boston, MA 2011).

[31] S. Kojima and H. Takeda, "Sit-to-stand movement in elderly adults," *Rigakuryoho Kagaku* **13**(2), 85–88 (1998). doi: 10.1589/rika.13.85.

[32] W. G. Janssen, H. B. Bussmann and H. J. Stam, "Determinants of the sit-to-stand movement: A review," *Phys. Ther.* **82**(9), 866–879 (2002).